Hypoxic postconditioning reduces microglial activation, astrocyte and caspase activity, and inflammatory markers after hypoxia–ischemia in the neonatal rat brain

Jonathan D. Teo[1], Margaret J. Morris[1] and Nicole M. Jones[1]

BACKGROUND: Postconditioning (PostC) with mild hypoxia shortly after a neonatal hypoxic–ischemic (HI) brain injury can reduce brain damage, however, the mechanisms underlying this protection are not known. We hypothesize that hypoxic PostC reduces brain markers of glial activity, inflammation, and apoptosis following HI injury.

METHODS: Sprague Dawley rat pups were exposed to right common carotid artery occlusion and hypoxia (7% oxygen, 3 h) on postnatal day 7 and 24 h later, pups were exposed to hypoxic PostC (8% O_2 for 1 h/day for 5 d) or kept at ambient conditions for the same duration. HI+N pups demonstrated ~10% loss in ipsilateral brain tissue which was rescued with HI+PostC. To investigate the cellular responses, markers of astrocytes, microglia, inflammation, and caspase 3 activity were examined using immunohistochemistry and enzyme-linked immunosorbent assay.

RESULTS: PostC reduced the area of astrocyte staining compared to HI+N. There was also a shift in microglial morphology toward a primed state in both PostC groups. Protein levels of interleukin-1β and caspase 3 were elevated in HI+N brains and reduced by PostC.

CONCLUSION: This is the first demonstration that PostC can reduce glial activity, inflammatory mediators, and cell death after a neonatal HI brain injury.

Neonatal hypoxic–ischemic (HI) brain injury is a primary cause of neonatal mortality due to lack of oxygen and blood flow to the brain, causing approximately one million neonatal deaths every year (1). Currently, the only clinical treatment available for these infants is hypothermia, which has limited success in reducing mortality and neurodevelopmental disabilities (2). Thus, there is a need to develop additional therapeutic strategies to minimize brain damage and potentially promote brain repair after HI.

After HI injury, microglial activation occurs, followed by the release of inflammatory mediators, including the cytokines interleukin (IL)-1β and tumor necrosis factor α (TNF-α). Levels of IL-1β increase after HI (3) and excitotoxic brain injury can be reduced by an IL-1β receptor antagonist in newborn rats (4). Similarly, TNF-α and IL-1β gene expression in the brain were increased after a systemic inflammatory and central excitotoxic insult in neonatal mice and this was reduced in TNF-α knockout mice and by TNF-α blockade using etanercept (5). Preventing microglial activation with minocycline reduced levels of IL-1β, TNF-α, and restricted brain tissue loss after HI in the neonatal rat (6). These studies suggest that microglial activation and proinflammatory mediators play an important role in mediating brain injury responses and moderating inflammatory responses can reduce the extent of injury.

Astrocytes have important roles in blood–brain barrier function, metabolism, uptake of glutamate, and the formation of a glial scar during injury. Studies using glial fibrillary acid protein (GFAP) and vimentin knockouts have shown that reactive gliosis surrounding a lesion site can protect against injury and delay functional recovery following stroke in mice (7,8). There is substantial evidence suggesting that astrocyte activation can inhibit normal restorative processes at later stages of injury to the adult central nervous system (9,10). In the neonatal brain, preventing astrogliosis by knocking out these intermediate filaments did not affect the overall brain injury but increased cortical neurogenesis after HI, highlighting the complex role of astrocytes in normal and pathological processes in the brain (11). Therefore, in the developing brain, regulating astrocyte activity might offer beneficial effects after an HI brain injury.

Delayed cell death is involved in neuronal pruning, which is an important process that occurs in the brain during development (12). In the progression of HI injury, apoptosis closely follows necrosis which happens due to energy failure. Apoptosis is triggered by a cascade of proapoptotic initiator and effector caspase activity, caspase 3 in particular (13). Pharmacological inhibitors of apoptosis can reduce damage (14) and improve sensorimotor function in neonatal models of brain injury (15). Hence, reducing apoptosis by limiting caspase 3 activity might prove to be a viable target in reducing the injury sustained as a result of neonatal HI injury.

Previous studies showed that mild hypoxic preconditioning reduced tissue loss following HI in the neonatal rat brain (16,17), and this protection may be mediated by reduced

[1]Department of Pharmacology, School of Medical Sciences, University of New South Wales, New South Wales, Australia. Correspondence: Nicole M. Jones (n.jones@unsw.edu.au)

Received 15 May 2014; accepted 12 November 2014; advance online publication 1 April 2015. doi:10.1038/pr.2015.47

apoptosis and inflammatory mediators (18,19). While animal studies have shown robust protective effects of hypoxic preconditioning, the bench to bedside application remains limited due to the unpredictable nature of HI brain injury in human newborns. Recent studies have shown neuroprotective effects after exposure to hypoxic postconditioning (PostC) following a brain injury in rodents (20,21). The current study investigates the potential mechanism of neuroprotection by hypoxic PostC after a neonatal HI brain injury in rats. Here, we have examined the response of different brain cell populations including neurons, microglia, astrocytes, and inflammatory mediators in the cortex of the brain following PostC and HI.

RESULTS

Effects of Hypoxic PostC on Brain Tissue Loss After HI Injury in the Neonatal Rat

Utilizing the Rice-Vannucci model of unilateral HI brain injury in the neonatal rat (16), brain tissue loss was examined 7 d postinjury, on postnatal day 14 (P14), in the first set of experiments using cresyl violet (CV) staining. Throughout the

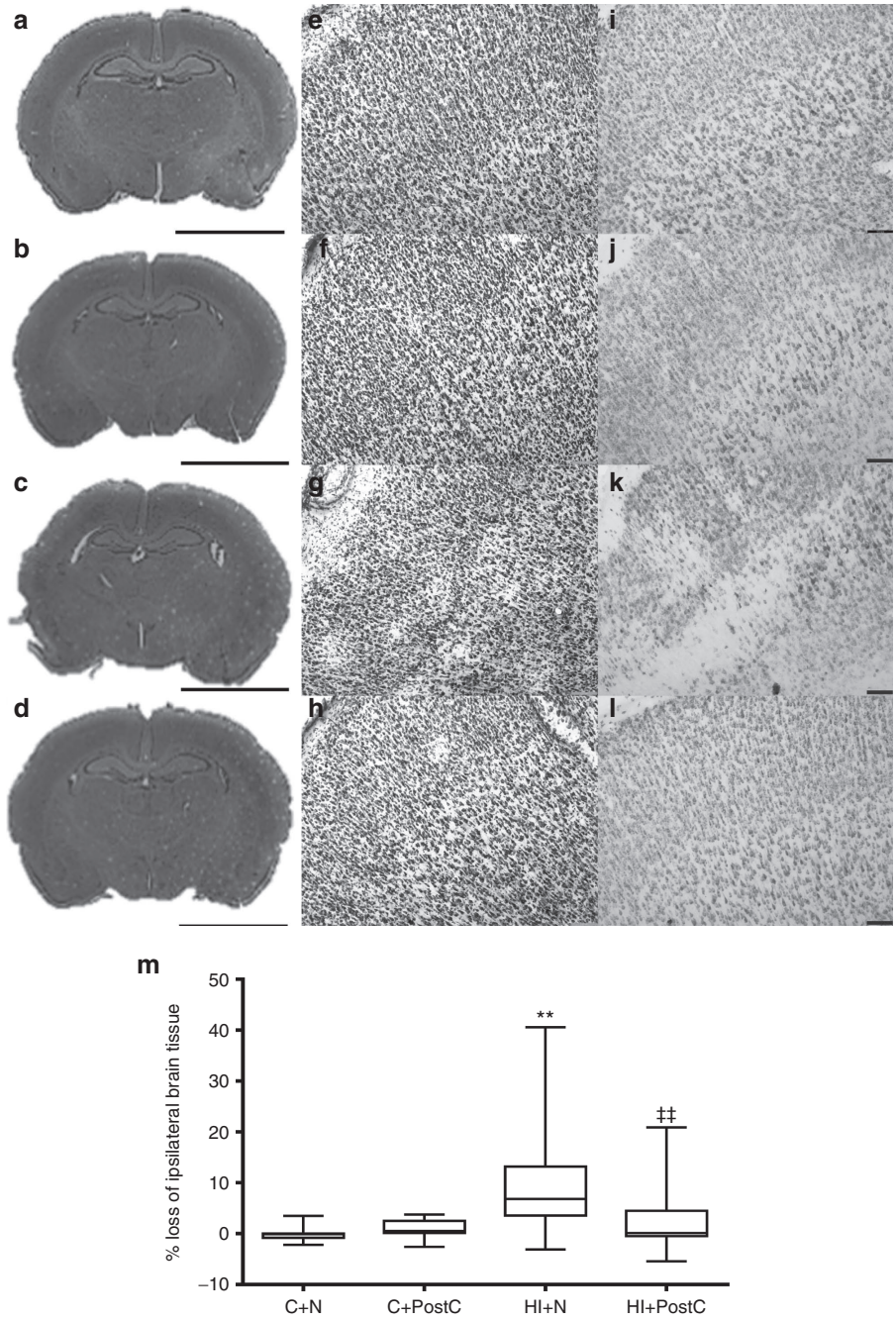

Figure 1. Representative images and quantification of brain tissue loss using cresyl violet and NeuN staining from P14 rat pup sections. Images from C+N (**a,e,i**), C+PostC (**b,f,j**), HI+N (**c,g,k**), and HI+PostC (**d,h,l**) treatment groups are presented. (**m**) Brain tissue loss in the ipsilateral hemisphere compared to the contralateral hemisphere is expressed as a percentage for C+N ($n = 8$), C+PostC ($n = 8$), HI+N ($n = 15$), and HI+PostC ($n = 16$). Values are median with min and max range. $^{**}P < 0.01$ vs. C+N, $^{‡}P < 0.05$ vs. HI+N by Kruskal–Wallis followed by Dunn's multiple comparison test. Scale bar: **a–d** = 0.5 cm; **e–l** = 100 µm.

experiment, pup weights were monitored and were not different between the treatment groups at the end of the experiment (~21 g). Histological staining of the neonatal rat brain using CV indicates tissue loss in the brain hemisphere ipsilateral to the carotid artery occlusion (**Figure 1c**), with the most consistent damage occurring in the cortex (**Figure 1g**) when compared to controls (C+N; **Figure 1a**,**e**) and hypoxic PostC alone (C+PostC; **Figure 1b**,**f**). HI-induced brain injury was reduced by hypoxic PostC (**Figure 1d**) with smaller, sporadic tissue loss observed (HI+PostC; **Figure 1h**). Further investigation of the HI injury using NeuN immunohistochemistry reveals neuronal loss in the ipsilateral cortex (**Figure 1k**) compared to controls (**Figure 1i**,**j**). HI+PostC reduced the neuronal loss with NeuN-positive staining observed consistently through the cortex, similar to control animals. Quantitative analysis of brain tissue loss in the ipsilateral hemisphere across treatment groups (**Figure 1m**) found that HI+N pups had a significant loss of brain tissue compared to the C+N group ($P < 0.005$). HI+PostC was able to reduce this tissue loss compared to HI+N ($P < 0.01$). No significant brain tissue loss was observed in the C+N and C+PostC groups.

Effects of Hypoxic PostC on Glial Response After HI Injury in the Neonatal Rat

To study the effects of HI and PostC on the brain glial response, P14 brain sections were stained for astrocytes using an antibody for GFAP. HI+N brains showed more hypertrophic astrocytes with denser staining and enlarged branches (**Figure 2c**), compared to the control group (**Figure 2a**). Following HI+PostC, there was a reduced glial reaction in response to the injury, where astrocytes were not as heavily stained with GFAP and had thinner processes (**Figure 2d**), which was similar to C+PostC (**Figure 2b**). Quantitative analysis of the GFAP-positive stained area in the ipsilateral somatosensory cortex (**Figure 2e**) indicates that astrocytes are more hypertrophic in the HI+N group compared to control ($P < 0.05$). Following HI+PostC, there was a reduction in the overall area of GFAP staining compared to HI+N, back to control levels. There was no difference in GFAP-stained area in the C+N and C+PostC groups. GFAP staining in the brain from C+PostC and HI+PostC groups appeared to have more staining present in the area around the blood vessels (**Figure 2b**,**d**).

Effects of Hypoxic PostC on Microglial Activation After HI Injury in the Neonatal Rat

Sections were stained with an antibody for Iba-1 to study the effects HI and PostC on microglial activation 1 wk postinjury, on P14. HI+N rats displayed more amoeboid microglia in the ipsilateral cortex with large, dense cell bodies and shorter (with at most two) processes (**Figure 3c**) compared to the other treatment groups. HI+PostC (**Figure 3d**) reduced the amoeboid phenotype of microglial activation back to control levels. In the control group, the predominant microglia appeared to have a ramified phenotype, with mostly small cell bodies and long surveying processes (**Figure 3a**,**b**). Throughout all of the treatment groups, the total number of microglia in

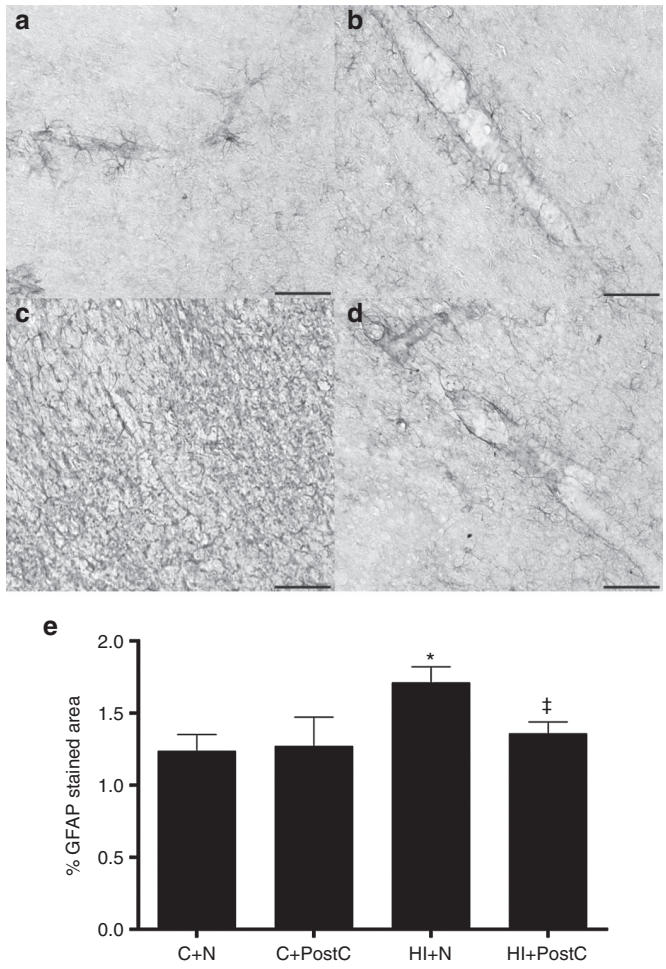

Figure 2. Representative images and quantification of gliosis using GFAP immunohistochemistry from P14 rat pup sections. The ipsilateral somatosensory cortex was photographed in C+N (**a**), C+PostC (**b**), HI+N(**c**), and HI+PostC (**d**) treatment groups. (**e**) Quantification of GFAP staining is expressed as a percentage of the whole area for C+N ($n = 8$), C+PostC ($n = 8$), HI+N ($n = 15$), and HI+PostC ($n = 16$) animals. Values are mean ± SEM. *$P < 0.05$ vs. C+N, ‡$P < 0.05$ vs. HI+N, by one-way ANOVA and Fisher's least significant difference test. Scale bars: 100 μm.

the micrographs was similar (data not shown). Quantitative analysis of the proportion of microglia of each phenotype (**Figure 3e**), indicated that C+N animals had mostly ramified microglia with less primed and the least amount of amoeboid microglia. C+PostC animals had less ramified ($P < 0.005$) and more primed ($P < 0.01$) microglia compared to C+N. HI+N animals had the most amoeboid and least ramified microglia compared to C+N ($P < 0.001$). HI+PostC animals had more ramified ($P < 0.05$) and primed ($P < 0.001$) and less amoeboid ($P < 0.001$) microglia compared to HI+N but still had less ramified microglia compared to C+N ($P < 0.001$).

Effects of Hypoxic PostC on Inflammatory Cytokines After HI Injury in the Neonatal Rat

A new cohort of animals that underwent the same HI and PostC procedure was generated and fresh brain tissue was collected for protein analyses. Protein levels of proinflammatory

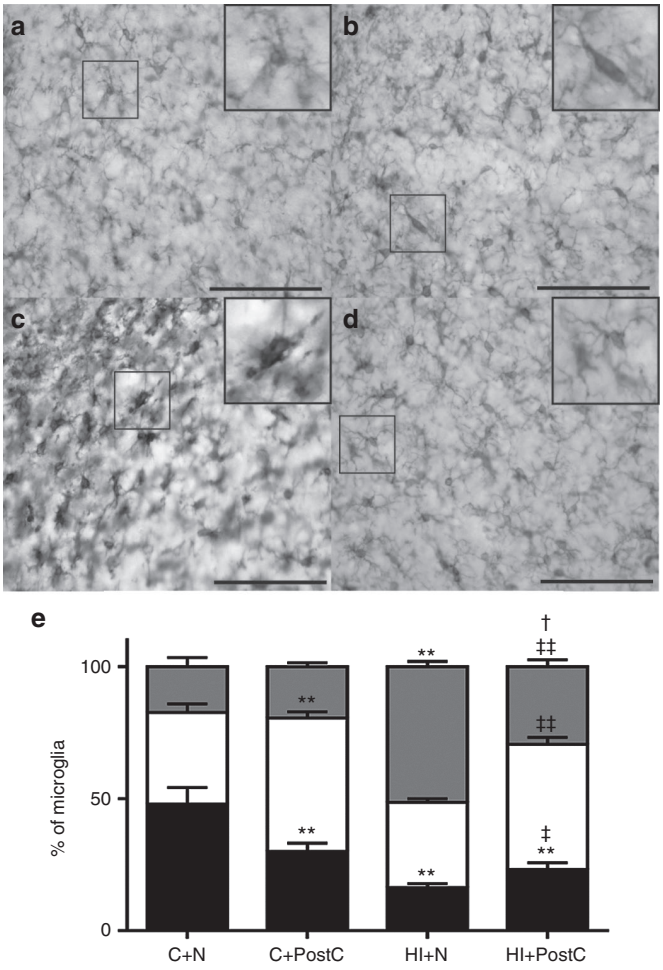

Figure 3. Representative images and quantification of microglial activity using Iba-1 immunohistochemistry from P14 rat pup sections. The ipsilateral somatosensory cortex was photographed in C+N (**a**), C+PostC (**b**), HI+N (**c**), and HI+PostC (**d**) groups. Higher magnification images of the microglia that displayed ramified (**a**), primed (**b** and **d**) and amoeboid (**c**) morphologies were included as insets in each panel. (**e**) Quantification of the three main microglial phenotypes (amoeboid in gray, primed in clear, and ramified in black boxes) was performed and the data are expressed as a percentage of the total number of microglia in each micrograph for C+N ($n = 8$), C+PostC ($n = 8$), HI+N ($n = 15$), and HI+PostC ($n = 16$). Values are mean ± SEM. $^{**}P < 0.01$vs. C+N, $^{‡‡}P < 0.01$ vs. HI+N, $^{†}P < 0.05$ vs. C+PostC by two-way ANOVA and Fisher's least significant difference test. Scale bars = 100 µm.

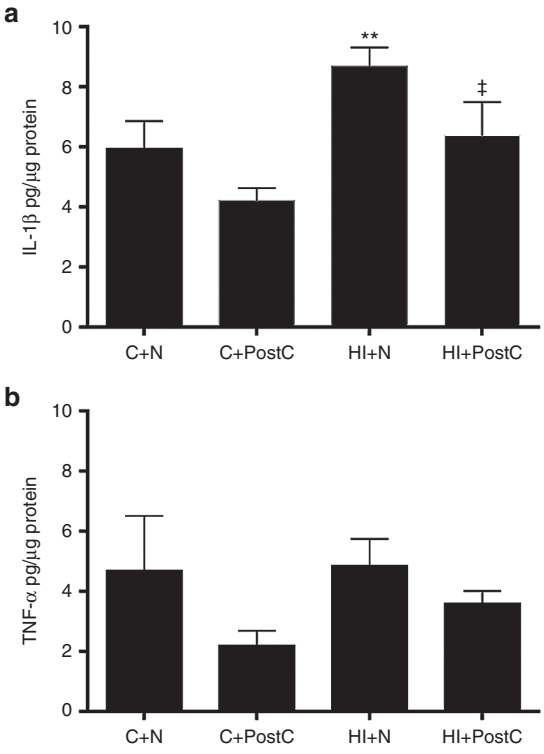

Figure 4. Inflammatory markers, IL-1β and TNF-α after HI and PostC. Protein levels of IL-1β (**a**) and TNF-α (**b**) measured using enzyme-linked immunoabsorbance assay in tissue from the ipsilateral cortex of P12 rat pups from C+N ($n = 3$), C+PostC ($n = 3$), HI+N ($n = 11$), and HI+PostC ($n = 12$) treatment groups. Values are mean ± SEM. $^{**}P < 0.01$ vs. C+N, $^{‡}P < 0.05$ vs. HI+N by Mann–Whitney *U*-test.

mediators, IL-1β and TNF-α were measured using enzyme-linked immunoabsorbance assay (ELISA), in tissue homogenates prepared from the ipsilateral cortex at 5 d post-HI. There was a significant increase in IL-1β levels (**Figure 4a**) in HI+N pups compared to the controls ($P < 0.01$). PostC after HI significantly reduced the elevated levels of IL-1β protein levels in the ipsilateral cortex ($P < 0.05$) compared to HI+N animals, and PostC alone had no effect on IL-1β levels. Analysis of TNF-α protein levels did not show any significant differences across the treatment groups (**Figure 4b**, $P > 0.05$).

Effects of Hypoxic PostC on Active Caspase 3 Staining in Neurons After HI Injury in the Neonatal Rat

Caspase 3 colocalization with NeuN was measured in P14 sections to examine the effects of HI and PostC on neuronal apoptosis. Immunofluorescent staining in the ipsilateral somatosensory cortex revealed disorganized neuronal layers and patchy NeuN staining (**Figure 5c**) and more active caspase 3 staining (**Figure 5g**) in the HI+N animals compared to the NeuN and active caspase 3 staining in the C+N (**Figure 5a**,**e**) and C+PostC (**Figure 5b**,**f**) groups. HI+PostC was able to protect against neuronal loss (**Figure 5d**) and appeared to reduce active capase 3-positive cells (**Figure 5h**). Colocalization of the two markers did not show any difference between the C+N (**Figure 5i**) and C+PostC (**Figure 5j**) groups. HI+N appeared to have more colocalized caspase 3 and NeuN (**Figure 5k**) compared to the controls which was not as extensive in the HI+PostC sections (**Figure 5l**), resembling the controls. Quantification of caspase 3-positive neurons (**Figure 5m**) confirmed a significant increase in the HI+N sections ($P < 0.001$) compared to C+N. When PostC was given after HI, the number of caspase 3-positive neurons was significantly reduced ($P < 0.05$) compared to the HI+N. No difference in the number of colocalized cells was detected between the control groups.

DISCUSSION

Our study has shown that mild hypoxia given after a neonatal HI brain injury in rats reduced brain tissue loss, and is the first to suggest that the neuroprotection offered from hypoxic PostC might be mediated by moderating glial activity, inflammation, and apoptosis. In line with previous studies using the

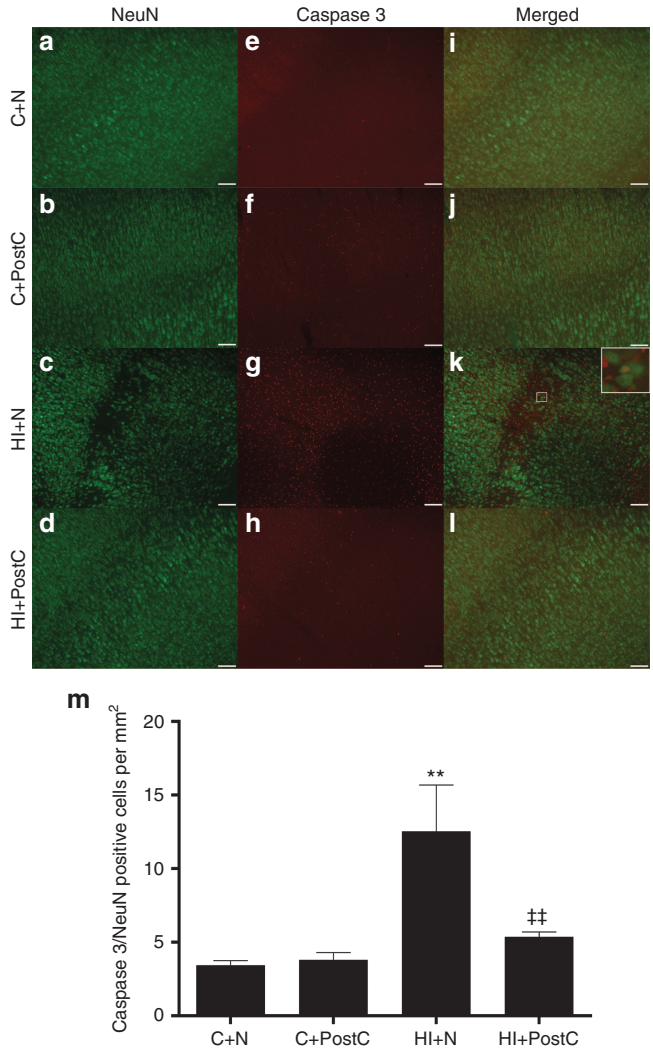

Figure 5. Representative images and quantification of active caspase 3 and NeuN immunohistochemistry from P14 rat pup sections were stained with NeuN (green) and active Caspase 3 (red). The ipsilateral somatosensory cortex was photographed from the C+N (**a,e,i**), C+PostC (**b,f,j**), HI+N (**c,g,k**), and HI+PostC (**d,h,l**) treatment groups. Cells which demonstrated colocalized active caspase 3 and NeuN staining (inset K) within the area of the merged micrographs were counted for pups from C+N ($n = 8$), C+PostC ($n = 8$), HI+N ($n = 15$), and HI+PostC ($n = 16$) animals (**m**). Values are mean ± SEM. $^{**}P < 0.01$ vs. C+N, $^{‡‡}P < 0.01$ vs. HI+N, using a Kruskal–Wallis followed by Dunn's multiple comparison test. Scale bar = 100 µm.

Rice-Vannucci model of neonatal HI brain injury (16,22,23), we have demonstrated a significant injury in the ipsilateral hemisphere with heightened glial and inflammatory responses after HI. PostC with mild hypoxia was first shown to be neuroprotective in primary neuronal cultures and an adult rat model of middle cerebral artery occlusion (21). Recently, we have shown that hypoxic PostC reduced cortical and striatal neuronal injury after HI in neonatal rats (20). Our data confirm that hypoxic PostC reduced brain tissue loss after neonatal HI and further investigated the cellular responses of the brain to mild hypoxia.

Necrosis and programmed cell death are the main two pathways of cell death that account for cell loss following neonatal HI brain injury. Active caspase-3 is the protein that executes programmed cell death and removes unnecessary neurons (24). Necrosis is a rapid process that occurs minutes to hours after the initial insult, peaking around 12 h after injury (25). The protective effect of hypoxic PostC was observed when initiated 24 h after HI, following the initial necrotic phase, hence we explored the effect of PostC on active caspase 3 to assess potential effects on apoptosis. Our study clearly showed a marked increase in active caspase 3 and decreased NeuN staining in HI+N animals. HI+PostC reversed these effects. The processes involved in the progression of HI injury are complicated, especially in the neonatal rat brain. The concept of excitotoxic neuronal death has been thought of as being a continuum of cell death involving apoptosis, necrosis, and intermediate forms of cell death (26) and targeting one specific pathway, such as with the use of caspase inhibitors, may merely shift cell death toward the necrotic route (27). This highlights the importance of our observations. By using two indicators of cell death, we found that hypoxic PostC not only reduced caspase 3-mediated cell death, but may also prevent a shift to other paths of cell death such as aponecrosis, leading to brain tissue preservation after HI. Previous studies have shown that using hypoxic preconditioning can prevent HI-induced increase in terminal deoxynucleotidyl transferase dUTP nick-end labeling staining in neonatal rats and found increased expression of antiapoptotic and downregulation of proapoptotic genes, supporting the use of mild hypoxia as a viable inhibitor of apoptosis (18).

In response to HI, astrocytes form a glial scar to encase the injury. Here, we observed a marked increase in gliosis after HI in comparison to the HI+PostC and C groups. Previous studies have indicated that reactive astrocytes are important for tissue remodeling after injury, and morphological changes in astrocytes, accompanied by an increased expression of GFAP as well as astrocyte proliferation have been observed in the ipsilateral hemisphere after neonatal HI (28). Hypoxic preconditioning has been shown to increase neocortical astrocyte maturation and differentiation, glial expression of excitatory amino acid transporters, glutamine synthetase, and glucose transporters that may contribute to the protective actions against a subsequent HI brain injury (17,29). On the other hand, preventing gliosis using GFAP and vimentin knockout mice had no effect on lesion size, but enhanced neurogenesis following neonatal HI brain injury (11). In light of these studies, our findings point to two possibilities—that hypoxic PostC is having an effect on gliosis thereby reducing injury or that PostC directly reduces injury, hence a less severe astrocyte response. We have observed that astrocytes in both PostC groups were predominantly localized around the blood vessels compared to the control. This suggests that a mechanism for PostC induced neuroprotection might be by enhancing the interaction between astrocytes and the potential protection of the blood–brain barrier. A recent study showed that chronic hypoxia was able to induce the growth of blood vessels and elicit astrocyte adaptation around new blood vessels, thereby stabilizing the blood–brain barrier (30). Furthermore, reactive astrocytes were seen to reduce infarct volume after an ischemic brain injury in mice through glutamate uptake, astrocyte

gap junctional communication and possibly reconstruct the compromised blood–brain barrier (7). Preconditioning with hypoxia can increase hypoxia inducible factor-1 (HIF-1), the angiogenic factor, vascular endothelial growth factor (VEGF), and can reduce caspase 3 activity after HI thus protecting surrounding cells and vasculature in the neonatal brain (17,31). Taken together with our own observations, these studies indicate that mild hypoxia is likely to be beneficial against neonatal HI by influencing multiple glial responses such as enhancing astrocyte regulation of the blood–brain barrier and reducing gliosis.

Here, we observed distinct morphological changes in microglia across the different treatment groups. Following HI+N, the predominant microglia were of the amoeboid phenotype while the C+N animals had mainly ramified or surveying microglia. In both of the PostC groups, most microglia appeared to be in a primed state. In agreement with the morphological characteristics of the microglia observed in our study, microglia assume the more activated, amoeboid phenotype in response to an HI brain injury (32). When activated, microglia from neonatal rat brains can release neurotoxic factors and enhance cell death when cocultured with hypoxia-exposed neurons, suggesting that microglia might contribute to injury processes early in development (33). Reducing microglial activation using the anti-inflammatory drug, minocycline, can prevent neonatal HI brain injury (6). These studies support our hypothesis that hypoxic PostC has a protective effect by modulating microglial activation. Priming microglia using lipopolysaccharide before an injury has been seen to offer neuroprotection in different neonatal rodent models of brain injury and disease (34,35). The primed microglia seen following lipopolysaccharide, which have asymmetrical cell bodies and thicker processes compared to ramified microglia, bear similar morphology to the majority of microglia seen in our PostC treatment groups. Our results suggest that PostC can shift the microglia into a primed state from the ramified state observed in the C+N group and from the amoeboid state in the HI+N group. Aside from having less amoeboid microglia after the injury, microglia in the primed state might be releasing neuroprotective factors, such as neutrophins and brain-derived neurotrophic factor, which can directly contribute to reducing brain tissue loss (36,37).

We have also shown that levels of IL-1β protein were elevated in the ipsilateral cortex following HI and this was reduced with PostC with TNF-α levels following a similar trend. Previous studies have shown that brain levels of TNF-α and IL-1β peak at 24 h and TNF-α returns to basal levels after 48 h while IL-1β remains elevated until at least 72 h after neonatal HI (22). Therefore, it is likely that the lower levels of TNF-α and IL-1β we observed 5 d after HI had already started going down, suggesting that we might have missed the peak of release of both cytokines. Higher levels of proinflammatory cytokines are likely to exacerbate brain injury processes, where increased IL-1β and exogenous TNF-α relate to worse outcomes in rodent stroke models (5,38). IL-1β knockout mice demonstrate reduced injury and axonal plasticity after a spinal cord injury (38), and blocking TNF-α offers neuroprotection against inflammatory and excitotoxic insults in neonatal rats (5). The anti-inflammatory strategy of using minocycline can reduce levels of TNF-α and IL-1β and protect against HI brain injury in the preterm rat neonate (6). Taken together, these studies suggest that a balance in the levels of inflammatory mediators after HI is crucial, and PostC may be a viable way of affecting this process.

While further studies are required to uncover the molecular mechanisms involved in the response of the brain to hypoxic PostC following neonatal HI, our findings demonstrate that hypoxic PostC can alter a number of cellular responses after HI, leading to the improvement of cell survival. One potential mechanism by which this happens is likely to be through the induction of HIF-1 and its many prosurvival target genes and processes such as increased extracellular signal-regulated kinases 1/2 signaling, VEGF, glucose transporters and glycolysis (17,21,39). In addition, pharmacological inhibition of VEGF caused a reduction in proliferation and survival in astrocyte cultures after hypoxia and glucose deprivation. Hence, our observation of increased intensity of GFAP staining might be due to hypoxia-induced VEGF expression (40). Postconditioning with ischemia was also seen to offer beneficial effects after a middle cerebral artery occlusion in rats by increasing tight junction proteins and improving blood–brain barrier integrity (41). Furthermore, hypobaric hypoxia postconditioning was seen to reduce the oxidative stress caused by a neonatal rat brain injury while increasing antioxidant levels (42). The therapeutic potential of hypoxic PostC extends further than neonatal HI brain injury used in this study. Its ability to influence a multitude of processes such as glial activity, inflammation, and apoptosis, makes it a valuable approach for many different types of brain injuries.

MATERIALS AND METHODS

Animals

All animal experiments were performed in accordance with the code of practice of the National Health and Medical Research Council (Australia) and with the approval of the University of New South Wales Animal Care and Ethics Committee. The dams and pups were kept under a 12 h light/dark cycle at room temperature (23 ± 1 °C), with access to food and water *ad libitum*.

HI Injury Model

Seven-day-old (P7) Sprague Dawley rat pups were randomly assigned to the control group or HI injury, performed following the Rice-Vannucci model (16). Male (n = 28) and female (n = 19) pups were used in this experiment (~15 g) and data from both sexes were combined. Animals in the HI group were anesthetized with 1.5% isofluorane/98.5% oxygen mixture and kept on a heating mat (37 °C) throughout the procedure. A ventral midline incision was made in the neck to expose the right carotid artery, which was permanently occluded with an electrocautery device. The wound was sutured and pups returned to their dam for 1 h. The pups were then placed into a hypoxic chamber (BioSpherix, Lacona, NY; 7% oxygen in nitrogen, at 37 °C) for 3 h. Throughout the procedure, pups in the control group were removed from their dams for the same duration and kept on a heating mat (37 °C) in ambient conditions. Following the procedure, all pups were returned to their mother and monitored daily for the subsequent week. Two pups died during surgery due to excessive blood loss. All of the other pups survived the procedures were included in subsequent data analysis.

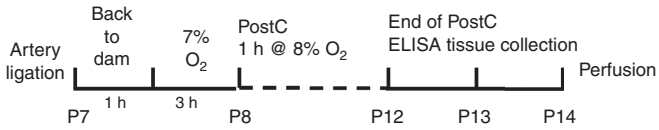

Figure 6. The experiment started on P7 when rat pups were randomly distributed to C or HI groups for right carotid artery occlusion. Pups were returned to their dam for 1 h before a 3-h exposure to 7% oxygen at 37 °C. Twenty-four hours after injury, pups were randomly assigned to N or PostC groups for 1 h exposure to 8% oxygen at 37 °C daily for 5 d. Fresh brain tissue was collected on P12 for enzyme-linked immunoabsorbance assays and fixed tissue was collected on P14 for immunohistochemistry.

Hypoxic PostC Treatment

Pups from the control and HI groups were then further assigned into normoxic (C+N; n = 8, HI+N; n = 15) or PostC (C+PostC; n = 8, HI+PostC; n = 16) groups. Twenty-four hours after HI surgery, pups were removed from their dam and placed in a hypoxic environment (8% oxygen with nitrogen, at 37 °C) or kept at ambient conditions on a heating mat for 1 h. This treatment occurred daily for the subsequent 5 d postinjury. These conditions have been previously shown to reduce brain tissue and neuronal loss (20,21) (**Figure 6**).

Histopathology and Morphological Staining

One week after HI injury, all rats were euthanized with pentobarbitone sodium (100 mg/kg, i.p.) and perfused transcardially with phosphate-buffered saline followed by 4% paraformaldehyde solution (**Figure 6**). This time course was previously shown to encompass brain damage due to all injury mechanisms (20). Sixty-micrometer rostro-caudal, serial coronal cryostat brain sections were collected and stored in a cryoprotectant (25% glycerol, 25% ethylene glycol, 50% phosphate-buffered saline).

CV Staining and Brain Injury Quantification

One series of free floating coronal sections (60 µm sections, 1,440 µm apart) from each animal were mounted onto slides and stained with 0.5% CV (Sigma-Aldrich, St Louis, MO) and scanned at low resolution using a HP LaserJet 3052 flatbed scanner. The volume of each hemisphere was measured using the ImageJ software (Bethesda, MD) by multiplying the area of the sections by the distance between each section. Brain tissue loss in the ipsilateral hemisphere was calculated as a percentage of the contralateral hemisphere.

Immunohistochemistry for Iba-1 and GFAP

Four coronal sections from each animal was selected from brain regions approximating Bregma 3.24, 1.20, −3.00, and −4.80 mm (43). Sections were exposed to sodium citrate antigen retrieval solution (10 mmol/l, pH 6.0, 70 °C) for 10 min and then blocked for 2 h at room temperature (5% skim milk powder, 0.1% bovine serum albumin, 0.3% triton X-100, 2% horse or goat serum in phosphate-buffered saline). The sections were incubated overnight at 4 °C with primary antibodies (mouse anti-GFAP (1:1,000; Millipore MAB360, Billerica, MA); mouse anti NeuN (1:1,000; Millipore MAB377); goat anti Iba-1 (1:1,000; Abcam ab5076, Cambridge, MA)) and then incubated with biotinylated secondary antibodies at room temperature for 2 h (1:200; Vector Lab BA-2001/BA-1000, Burlingame, CA and Millipore AP106B respectively), followed by horseradish peroxidase streptavidin (1:500, Vector SA-5004) for 2 h. For antibody visualization, diaminobenzidine (Vector SK-4100) was used. Negative controls were performed using the same procedure described above in the absence of the primary antibody. Sections were mounted, dehydrated, and coverslipped prior to imaging.

Quantitative Image Analysis of Immunohistochemical Staining

Following microscopic observations of the most consistent injury patterns in the somatosensory cortex, adjacent sections approximating Bregma 1.20 mm from each animal were chosen for image analysis of microglia and astrocytes the somatosensory cortex using an Olympus BX51 microscope, equipped with an MAC-6000 motorized stage controller and a 2000R-F-CLR-12-C-25 mm digital camera connected to a computer running StereoInvestigator v9 (all from MicroBrightField, Colchester, VT). Iba-1-stained microglia within each micrograph of the ipsilateral somatosensory cortex were counted based on their morphology, into three distinct categories (44). Ramified microglia had small circular cell bodies with highly ramified processes. Primed/reactive microglia had bigger and less round cell body with a few ramified processes while amoeboid microglia presented at most two unramified processes or were completely devoid of them. Astrocyte activation, revealed through GFAP-positive staining, was imaged in the same region of the somatosensory cortex with lens exposure set to 99% on the StereoInvestigator program. The area occupied by the GFAP staining was processed through ImageJ and expressed as a percentage of the total area of the micrograph.

Immunofluorescence for Caspase 3 and NeuN

To investigate caspase 3 colocalization in neurons in the same region assessed for microglia and astrocyte activity, two coronal sections approximating Bregma 1.20 mm were chosen for immunofluorescent staining. Sections were treated as described above before being incubated with primary antibodies (rabbit anti-Caspase 3 1:1,000; Millipore AB3623 and mouse anti-NeuN 1:1,000 Millipore MAB377) for 48 h at 4 °C, followed by incubation in 1:1,000 dilution of fluorescent secondary antibody (Alexa Fluor568 goat anti-rabbit; Invitrogen A-11036, , Victoria, Australia, Alexa Fluor488 goat anti-mouse; Invitrogen A11001) for 2 h in the dark at room temperature and mounted on microscope slides (SlowFade Gold Antifade reagent; Invitrogen S36936) and coverslipped prior to visualization.

Quantitative Image Analysis of Immunofluorescent Staining

Fluorescent images of active caspase 3 and NeuN double labeling were also captured in adjacent sections to allow comparison with the Iba-1 and GFAP staining and merged using ImageJ. Colocalized active caspase 3 and NeuN markers were counted and quantified.

ELISA

An additional cohort of animals underwent the procedures mentioned above (**Figure 6**; C+N = 3; C+PostC = 3; HI+N = 11; HI+PostC = 12; males = 15; females = 14). To measure cytokines prior to returning to basal levels, 5 d after injury, pups were euthanized with pentobarbitone sodium (100 mg/kg, i.p.) and brains were removed. Cortical tissue was homogenized in ice cold lysis buffer (20 mmol/l Tris-HCl (pH 7.5); 150 mmol/l NaCl; 1 mmol/l EDTA; 0.5% Triton X-100; 0.1% SDS) and centrifuged at 5,000 rpm × 2 min at 4 °C to remove cellular debris. Total protein concentration was determined using a commercial protein assay kit (Bio-Rad *DC* protein assay, Hercules, CA). Concentrations of IL-1β and TNF-α were determined using rat duoset ELISA kits (from 100 µg of protein per sample, in triplicate) according to the manufacturer's instructions (R&D systems, Minneapolis, MN). The absorbance values were read on a FLUROstar Optima plate reader (BMG LabTek, Ortenberg, Germany).

Data Analysis

All analyses were performed whereby the observer was blind to the experimental treatment. All statistical analyses were performed using PRISM 6 (PRISM 6, GraphPad, San Diego, CA) and results were evaluated using ANOVA followed by Fisher's least significant difference (LSD) or Kruskal–Wallis followed by Dunn's multiple comparison test or Mann–Whitney *U*-test for individual comparison. Data are presented as the mean ± SEM.

STATEMENT OF FINANCIAL SUPPORT

This study was supported by the University of New South Wales Silver Star Award, Australia.

Disclosure: The authors have nothing to disclose.

REFERENCES

1. Lawn J, Shibuya K, Stein C. No cry at birth: global estimates of intrapartum stillbirths and intrapartum-related neonatal deaths. Bull World Health Organ 2005;83:409–17.
2. Jacobs S, Berg M, Hunt R, Tarnow-Mordi W, Inder T, Davis P. Cooling for newborns with hypoxic ischaemic encephalopathy. Cochrane Database Syst Rev 2013;1.

3. Hedtjärn M, Leverin AL, Eriksson K, Blomgren K, Mallard C, Hagberg H. Interleukin-18 involvement in hypoxic-ischemic brain injury. J Neurosci 2002;22:5910–9.
4. Hagan P, Barks JD, Yabut M, Davidson BL, Roessler B, Silverstein FS. Adenovirus-mediated over-expression of interleukin-1 receptor antagonist reduces susceptibility to excitotoxic brain injury in perinatal rats. Neuroscience 1996;75:1033–45.
5. Adén U, Favrais G, Plaisant F, et al. Systemic inflammation sensitizes the neonatal brain to excitotoxicity through a pro-/anti-inflammatory imbalance: key role of TNFalpha pathway and protection by etanercept. Brain Behav Immun 2010;24:747–58.
6. Wixey JA, Reinebrant HE, Spencer SJ, Buller KM. Efficacy of post-insult minocycline administration to alter long-term hypoxia-ischemia-induced damage to the serotonergic system in the immature rat brain. Neuroscience 2011;182:184–92.
7. Li L, Lundkvist A, Andersson D, et al. Protective role of reactive astrocytes in brain ischemia. J Cereb Blood Flow Metab 2008;28:468–81.
8. Liu Z, Li Y, Cui Y, et al. Beneficial effects of gfap/vimentin reactive astrocytes for axonal remodeling and motor behavioral recovery in mice after stroke. Glia 2014;62:2022–33.
9. Wilhelmsson U, Li L, Pekna M, et al. Absence of glial fibrillary acidic protein and vimentin prevents hypertrophy of astrocytic processes and improves post-traumatic regeneration. J Neurosci 2004;24:5016–21.
10. Widestrand A, Faijerson J, Wilhelmsson U, et al. Increased neurogenesis and astrogenesis from neural progenitor cells grafted in the hippocampus of GFAP-/- Vim-/- mice. Stem Cells 2007;25:2619–27.
11. Järlestedt K, Rousset CI, Faiz M, et al. Attenuation of reactive gliosis does not affect infarct volume in neonatal hypoxic-ischemic brain injury in mice. PLoS One 2010;5:e10397.
12. Srinivasan A, Roth KA, Sayers RO, et al. In situ immunodetection of activated caspase-3 in apoptotic neurons in the developing nervous system. Cell Death Differ 1998;5:1004–16.
13. Wang X, Karlsson JO, Zhu C, Bahr BA, Hagberg H, Blomgren K. Caspase-3 activation after neonatal rat cerebral hypoxia-ischemia. Biol Neonate 2001;79:172–9.
14. Wang X, Han W, Du X, et al. Neuroprotective effect of Bax-inhibiting peptide on neonatal brain injury. Stroke 2010;41:2050–5.
15. Han W, Sun Y, Wang X, Zhu C, Blomgren K. Delayed, long-term administration of the caspase inhibitor Q-VD-OPh reduced brain injury induced by neonatal hypoxia-ischemia. Dev Neurosci 2014;36:64–72.
16. Rice JE 3rd, Vannucci RC, Brierley JB. The influence of immaturity on hypoxic-ischemic brain damage in the rat. Ann Neurol 1981;9:131–41.
17. Jones NM, Bergeron M. Hypoxic preconditioning induces changes in HIF-1 target genes in neonatal rat brain. J Cereb Blood Flow Metab 2001;21:1105–14.
18. Gustavsson M, Wilson MA, Mallard C, Rousset C, Johnston MV, Hagberg H. Global gene expression in the developing rat brain after hypoxic preconditioning: involvement of apoptotic mechanisms? Pediatr Res 2007;61:444–50.
19. Yin W, Signore AP, Iwai M, et al. Preconditioning suppresses inflammation in neonatal hypoxic ischemia via Akt activation. Stroke 2007;38:1017–24.
20. Galle AA, Jones NM. The neuroprotective actions of hypoxic preconditioning and postconditioning in a neonatal rat model of hypoxic-ischemic brain injury. Brain Res 2013;1498:1–8.
21. Leconte C, Tixier E, Freret T, et al. Delayed hypoxic postconditioning protects against cerebral ischemia in the mouse. Stroke 2009;40:3349–55.
22. Wang Y, Cao M, Liu A, et al. Changes of inflammatory cytokines and neurotrophins emphasized their roles in hypoxic-ischemic brain damage. Int J Neurosci 2013;123:191–5.
23. Pimentel VC, Pinheiro FV, De Bona KS, et al. Hypoxic-ischemic brain injury stimulates inflammatory response and enzymatic activities in the hippocampus of neonatal rats. Brain Res 2011;1388:134–40.
24. D'Amelio M, Cavallucci V, Cecconi F. Neuronal caspase-3 signaling: not only cell death. Cell Death Differ 2010;17:1104–14.
25. Garcia JH, Liu KF, Ho KL. Neuronal necrosis after middle cerebral artery occlusion in Wistar rats progresses at different time intervals in the caudoputamen and the cortex. Stroke 1995;26:636–42; discussion 643.
26. Portera-Cailliau C, Price DL, Martin LJ. Excitotoxic neuronal death in the immature brain is an apoptosis-necrosis morphological continuum. J Comp Neurol 1997;378:70–87.
27. Formigli L, Papucci L, Tani A, et al. Aponecrosis: morphological and biochemical exploration of a syncretic process of cell death sharing apoptosis and necrosis. J Cell Physiol 2000;182:41–9.
28. Sizonenko SV, Camm EJ, Dayer A, Kiss JZ. Glial responses to neonatal hypoxic-ischemic injury in the rat cerebral cortex. Int J Dev Neurosci 2008;26:37–45.
29. Sen E, Basu A, Willing LB, et al. Pre-conditioning induces the precocious differentiation of neonatal astrocytes to enhance their neuroprotective properties. ASN Neuro 2011;3:e00062.
30. Masamoto K, Takuwa H, Seki C, et al. Microvascular sprouting, extension, and creation of new capillary connections with adaptation of the neighboring astrocytes in adult mouse cortex under chronic hypoxia. J Cereb Blood Flow Metab 2014;34:325–31.
31. Feng Y, Rhodes PG, Bhatt AJ. Hypoxic preconditioning provides neuroprotection and increases vascular endothelial growth factor A, preserves the phosphorylation of Akt-Ser-473 and diminishes the increase in caspase-3 activity in neonatal rat hypoxic-ischemic model. Brain Res 2010;1325:1–9.
32. Sizonenko SV, Kiss JZ, Inder T, Gluckman PD, Williams CE. Distinctive neuropathologic alterations in the deep layers of the parietal cortex after moderate ischemic-hypoxic injury in the P3 immature rat brain. Pediatr Res 2005;57:865–72.
33. Lai AY, Dibal CD, Armitage GA, Winship IR, Todd KG. Distinct activation profiles in microglia of different ages: a systematic study in isolated embryonic to aged microglial cultures. Neuroscience 2013;254:185–95.
34. Chen Z, Jalabi W, Shpargel KB, et al. Lipopolysaccharide-induced microglial activation and neuroprotection against experimental brain injury is independent of hematogenous TLR4. J Neurosci 2012;32:11706–15.
35. Sawada H, Hishida R, Hirata Y, et al. Activated microglia affect the nigrostriatal dopamine neurons differently in neonatal and aged mice treated with 1-methyl-4-phenyl-1,2,3,6-tetrahydropyridine. J Neurosci Res 2007;85:1752–61.
36. Elkabes S, DiCicco-Bloom EM, Black IB. Brain microglia/macrophages express neurotrophins that selectively regulate microglial proliferation and function. J Neurosci 1996;16:2508–21.
37. Miwa T, Furukawa S, Nakajima K, Furukawa Y, Kohsaka S. Lipopolysaccharide enhances synthesis of brain-derived neurotrophic factor in cultured rat microglia. J Neurosci Res 1997;50:1023–9.
38. Boato F, Rosenberger K, Nelissen S, et al. Absence of IL-1β positively affects neurological outcome, lesion development and axonal plasticity after spinal cord injury. J Neuroinflammation 2013;10:6.
39. Jones NM, Bergeron M. Hypoxia-induced ischemic tolerance in neonatal rat brain involves enhanced ERK1/2 signaling. J Neurochem 2004;89:157–67.
40. Schmid-Brunclik N, Bürgi-Taboada C, Antoniou X, Gassmann M, Ogunshola OO. Astrocyte responses to injury: VEGF simultaneously modulates cell death and proliferation. Am J Physiol Regul Integr Comp Physiol 2008;295:R864–73.
41. Han D, Zhang S, Fan B, et al. Ischemic postconditioning protects the neurovascular unit after focal cerebral ischemia/reperfusion injury. J Mol Neurosci 2014;53:50–8.
42. Gamdzyk M, Makarewicz D, Słomka M, Ziembowicz A, Salinska E. Hypobaric hypoxia postconditioning reduces brain damage and improves antioxidative defense in the model of birth asphyxia in 7-day-old rats. Neurochem Res 2014;39:68–75.
43. Paxinos G, Watson C. The rat brain in stereotaxic coordinates. 6th edn. San Diego, CA: Academic Press, Elsevier, 2007.
44. Ayoub AE, Salm AK. Increased morphological diversity of microglia in the activated hypothalamic supraoptic nucleus. J Neurosci 2003;23:7759–66.